HHS Public Access

Author manuscript

*Proc SPIE Int Soc Opt Eng*. Author manuscript; available in PMC 2014 October 07.

Published in final edited form as:

*Proc SPIE Int Soc Opt Eng*. 2009 February 12; 7181: 71810M–. doi:10.1117/12.809868.

# An *in vivo* transmission electron microscopy study of injected dextran-coated iron-oxide nanoparticle location in murine breast adenocarcinoma tumors versus time

**A J Giustini**[1,2,*], **R Ivkov**[3,4], and **P J Hoopes**[1,2]

[1]Dartmouth Medical School, Hanover, NH 03755 USA

[2]Thayer School of Engineering, Dartmouth College, Hanover, NH 03755 USA

[3]Triton BioSystems, Inc., Chelmsford, MA 01824 USA†

## Abstract

Investigators are just beginning to use hyperthermia generated by alternating magnetic field (AMF) activated iron oxide nanoparticles (IONPs) as a promising avenue for targeted cancer therapy. An important step in understanding cell death mechanisms in nanoparticle AMF treatments is to determine the location of these nanoparticles in relation to cellular organelles. In this paper, we report on transmission electron microscopy (TEM) studies designed to define the position of 100 nm diameter dextran-coated iron oxide nanoparticles in murine breast adenocarcinoma (MTG-B)and human colon adenocarcinoma tumors propagated in mice.

**METHODS—**Iron oxide nanoparticles (5 mg/g tumor) were injected into intradermal MTG-B flank tumors on female C3H/HEJ mice and into HT-29 flank tumors on female Nu/Nu mice. The IONPs were allowed to incubate for various times. The tumors were then excised and examined using TEM.

**RESULTS—**In the MTG-B tumors, most of the nanoparticles reside in aggregates adjacent to cell plasma membranes prior to three hours post-injection. By four hours post injection, however, most of the nanoparticles have been endocytosed by the cells. At time periods after four hours post injection, few visible extracellular nanoparticles remain and intracellular nanoparticles have densely aggregated within endosomes. In the HT-29 tumor, however, endocytosis of nanoparticles has not progressed to the same extent as in the MTG-B tumors by four hours post injection.

**CONCLUSIONS—**The time at which most of the nanoparticles transition from being extracellular to intracellular in the MTG-B system appears to be between two and four hours. The HT-29 cells, however, display different and delayed uptake pattern. These data show that there are IONP uptake differences between tumor types (cell lines) and that, based on known uptake



[*]Corresponding author. andrew.j.giustini@dartmouth.edu. Phone: (603) 650-8548.

[4]Current address: Dept. of Radiation Oncology and Molecular Radiation Sciences, Johns Hopkins University School of Medicine, Baltimore, MD 21231-5678

8. FINANCIAL AND COMPETING INTERESTS DISCLOSURE

These studies are partially supported by Aduro BioTech (Berkeley, CA. Formerly Triton BioSystems) via donation of iron oxide nanoparticles.

kinetics, nanoparticle hyperthermia can be employed as an extracellular or intracellular modality. These data will be important in guiding future nanoparticle hyperthermia cancer treatments.

**Keywords**

Iron oxide nanoparticle; hyperthermia; tumor; cancer; transmission electron microscopy; IONP; MTG-B; HT-29

## 2. BACKGROUND

Hyperthermia has been used in clinical oncology for more than 100 years, and in a sophisticated manner (radio frequency-, microwave-, and ultrasound-inducted) for more than 40 years. The lack of temperature targeting in specific tissues, especially tumors, has limited the clinical effectiveness of hyperthermia. Iron oxide nanoparticle (IONP)-induced hyperthermia appears capable of overcoming this limitation.

Magnetic hyperthermia was first attempted on tumor tissue in 1957 by Gilchrist et al. With *in vitro* experiments that involved injecting 5 mg of 20-100 nm diameter $Fe_2O_3$ nanoparticles into lymph nodes (47 mg of $Fe_2O_3$ per gram of tissue) they were able to produce a temperature rise of 14 degrees C in an AMF of 200-240 Oe at 1.2 MHz[1].

Although this use of IONPs to generate heat is promising, directing the IONPs to the tumor cells and away from normal tissue remains a significant challenge.

Due to the excellent biocompatibility of iron oxide nanoparticles particles[2], they have already been approved for animal and human studies in a number of settings. There are two types of dextran-coated IONPs being used in biological systems. The first are those nanoparticles typically used as imaging contrast agents, such as the ferumoxide Feridex[3]. The second are those particles that have been optimized for heating purposes[4]. The IONPs we are utilizing in these studies are of the latter type.

In order to better understand the cytotoxic mechanisms of interstitial nanoparticle hyperthermia within tumors, studies of uptake of nanoparticles by different tumor types and over different periods of time must be undertaken. Jordan, et. al. have undertaken *in vitro* studies to determine particle position within tumor cells versus time using silan- and dextran-coated iron oxide nanoparticles[5]. Studies of uptake in tumors, however, may give a more complete understanding of the uptake kinetics of dextran-coated iron oxide nanoparticles i*n vivo* in clinical oncology settings.

## 3. MATERIALS AND METHODS

### 3.1 Iron Oxide Nanoparticles

Dextran-coated BNF iron oxide nanoparticles (Lots # 1350684G and # 0340784-04) with an average hydrodynamic diameter of 95-140 nm (manufactured by MicroMod GmBH, Rostock, Germany) were used in a therapeutic suspension with an iron concentration of 14.5 mg/ml. The structure of the nanoparticles is that of iron-oxide core with a dextran shell.

### 3.2 MTG-B Tumors

MTG-B murine breast adenocarcinoma cells[6] were grown in Eagle's Minimum Essential Medium (MEM) with 10 % fetal bovine serum, 1% L-glutamine, and 1% penicillin-streptomycin. Cells were trypsinized and counted by staining with trypan blue dye and using a hemocytometer for counting of cells excluding the dye. The cells were then resuspended in 1x Alpha MEM at a concentration of 10 million cells per milliliter. Of this solution, 100 microliters per injection site were injected intradermally into the flanks of female C3H/HEJ mice (purchased from Charles River Laboratory) with a 25-gauge needle. Tumors were then allowed to grow until they reached a volume of 100 $mm^3$ +/− 50 $mm^3$, as determined by measuring three perpendicular diameters ($d_1$, $d_2$, $d_3$) of the tumors with calipers and calculating the volume with the equation for the volume of an ellipsoid:

$$Tumor \quad Volume = \frac{\pi \cdot d_1 \cdot d_2 \cdot d_3}{6}$$

This study was approved by the Dartmouth College Institutional Animal Care and Use Committee (IACUC) and was conducted in accordance with all federal Association for Assessment and Accreditation of Laboratory Animal Care (AAALAC) and institutional research guidelines.

### 3.3 HT-29 Tumor

HT-29 human colon adenocarcinoma cells were purchased from ATCC and grown in McCoy's 5A Medium with L-glutamine, 10% fetal bovine serum, and 1% penicillin-streptomycin. Cells were trypsinized and counted by staining with trypan blue dye and using a hemocytometer for counting of cells excluding the dye. The cells were then resuspended in Alpha MEM at a concentration of 50 million cells per milliliter. Using a 25-gauge needle and a syringe, 100 microliters were injected intradermally into the right flank of a female Nu/Nu mouse (purchased from Charles River Laboratory) with a 25-gauge needle. This tumor was allowed to grow until it reached a size of 125 $mm^3$, as determined by measuring three perpendicular diameters of the tumor with calipers and calculating the volume with the equation for the volume of an ellipsoid (shown above).

### 3.4 Nanoparticle Injection and Sample Retrieval

Upon reaching a tumor size of approximately 100 $mm^3$ +/− 50 $mm^3$, the mice were anesthetized with a ketamine (100 mg/kg) and xylazine (5 mg/kg) solution and nanoparticles were injected into the center of a tumor with a 30-gauge needle. The volume of the injection was chosen so than an iron concentration within the tumor of 5 mg Fe/g tumor tissue could be obtained. After a pre-determined time period post injection (for the MTG-B tumors: 5 minutes, 30 minutes, 1 hour, 2 hours, 3 hours, 4 hours, 9 hours, 13 hours, 18 hours, 22.5 hours, 5 days; for the HT-29 tumor: 4 hours) after injection, the mice were sacrificed and their tumors excised. Several 1 $mm^3$sections were harvested from each tumor and fixed in 4% glutaraldehyde solution. The samples were then washed three times with a sodium cacodylate buffer solution and kept in buffer until processing at the Dartmouth Electron Microscopy core facility. There was one tumor examined at each time point.

### 3.5 Transmission Electron Microscopy Preparation

Tumor samples were fixed in 4% glutaraldehyde in 0.1 Molar sodium cacodylate buffer (pH 7.4) overnight. The samples were then washed three times with 0.1 M sodium cacodylate buffer solution. Once at the TEM facility, the samples were post-fixed in osmium tetroxide in 0.1 M sodium cacodylate buffer. After several more wash cycles in sodium cacodylate buffer and distilled water, the samples were en-block stained in 2% uranyl acetate (aqueous) for one hour. After another distilled water wash cycle, the samples were dehydrated in various aqueous ethanol solutions (50% to 100% ethanol) and then in propylene oxide (PO). All reagents were received from, or used at, the Dartmouth Electron Microscopy core facility. Reagents were purchased from Ted Pella, Inc and Polysciences, Inc. The samples were then transferred through several PO and resin washes (Epon or LR White) until they were embedded in resin overnight in an oven to polymerize at 65 degrees C.

Once the samples were polymerized, thick sections (0.5 micron) were taken to confirm presence of cells. Then, thin sections (100 nm) were cut from the polymer blocks using a microtome. The samples were then viewed using a FEI Company Tecnai F20 FEG TEM operating at 100 kV.

## 4. RESULTS

### 4.1 MTG-B Tumors

At incubation times of less than 3 hours post-injection (Figure 1), virtually all nanoparticles seen in the sample are present as aggregates in the interstitial space between cells. Between 2 and 4 hours post-injection, particles are present in the interstitial space on cellular membranes and within the cells (Figure 2). At incubation times of 4 hours or greater, the great majority of the IONP seen are located within cells (Figures 3 and 4).

### 4.2 HT-29 Tumors

The preliminary data from this one tumor sample show that upon examination with TEM, few nanoparticles are seen to have been taken up by cells four hours post injection of nanoparticles into the tumor (Figures 4 and 5).

## 5. DISCUSSION

These preliminary data suggest IONP uptake in *in vivo* cancer cells are reasonably rapid and that there appears to be a distinct uptake difference between cell types: i.e the majority of IONP were intracellular by 4 hours post injection in MTG-B tumor cells. It is clear that MTG-B breast cancer cells readily take up IONPs and that this process begins very soon after IONP injection into the tumor mass. Although less well documented, it appears the primary IONP uptake process is largely complete within 6-8 hours post direct tumor injection. Nanoparticles are being taken up by cells and this process is time-dependent. The mechanism of cellular uptake of nanoparticles must be further explored in order to understand why different tumors have different uptake kinetics and how the anatomic positioning and ultrastructural relationship of the particles will affect IONP induced cytotoxicity and tumor treatment effect.

The extracellular membrane associated IONPs and intracellular IONPs are a result of different time-dependent domains of nanoparticle uptake by tumors and likely allow for different mechanism of cell killing in tumors when exposed to AMF. Since the nanoparticles act as the heating foci in nanoparticle hyperthermia therapy, having nanoparticles present inside of cells and adjacent to cellular organelles may lead to different types of cell damage than that which occurs when the nanoparticles are adjacent to the plasma membrane of the cells.

All of the images shown in the Figures 1 through 6 are representative of images from the various time endpoint studies acquired during TEM examination of the samples. In the *in vivo* MTG-B tumors, the transition from particles being located predominantly in the extracellular space to the intracellular space happens at approximately three hours. In the HT-29 tumor, however, this transition has not yet occurred by four hours post injection. Both of these tumor lines were adenocarcinomas, however one type was a human colon cancer line inoculated into athymic, nude mice and the other a murine breast cancer line in C3H mice. The difference in distribution of particles at each four hour time point implies different uptake kinetics in the two tumor lines. These tumor lines were chosen because they display similar *in vitro* doubling times (of approximately 24 hours) and are both adenocarcinomas. Since *in vitro* doubling time can be a surrogate measure for metabolic activity, it can be inferred from these data that metabolic activity may not be the only variable in cell lines affecting the kinetic properties of the uptake of dextran-coated nanoparticles.

One hypothesis that may account for the difference in uptake kinetics is the difference in the rate of cell cycling present in the two cell lines. While both cell lines displayed similar *in vitro* growth kinetics with similar doubling times of approximately 24 hours, the MTG-B tumors reached the 100 $mm^3$ size *in vivo* much more rapidly than did the HT-29 cells. The MTG-B tumors reached this size in approximately two weeks while the HT-29 tumor required approximately three weeks to achieve this volume. This more-rapid growth occurred despite there being 5-fold more HT-29 cells inoculated into the mice than MTG-B cells. This difference in growth kinetics implies more rapid progress through the cell cycle for MTG-B-derived tumors than for HT-29-derived tumors. This infers that the higher cell cycling rate correlates to more rapid uptake of IONPs. Additional studies to confirm the correlation between cell cycling rate and uptake of IONPs will be necessary.

A number of animal-based variables should also be considered when evaluating these *in vivo* studies. Nude (Nu/Nu) mice and C3H mice are different in many respects, most notably in the lack of a thymus and in the dearth of T cells within the Nu/Nu mice. Although the Nude mouse / immune system difference in our tumor models may not be a factor in INOP uptake kinetics (since the cancer cells themselves should be largely responsible for IONP uptake), one should not disregard the effect of the tumor stroma on extracellular activity and the fact that tumor stroma is derived from the host animal. Therefore the differences between syngeneic and xenograft models could help explain the difference in *in vivo* growth kinetics observed between the MTG-B and HT-29 tumors. Although both tumor lines were adenocarcinomas, one originated within a murine mammary gland and the other in a human

colon. It is unknown how the differences in tissue origin or species of tumor cell line would affect the uptake kinetics of the tumor.

## ACKNOWLEDGEMENTS

The authors would like to thank Katherine Connolly and Chris Ogomo at the Dartmouth Electron Microscopy Facility for their assistance with sample preparation and TEM imaging.

## REFERENCES

1. Gilchrist RK, Medal R, Shorey WD, Hanselman RC, Parrott JC, Taylor CB. Selective inducting heating of lymph nodes. Ann. Surg. 1957; 146:596–606. [PubMed: 13470751]
2. Pradhan P, Giri J, Samanta G, et al. Comparative evaluation of heating ability and biocompatibility of different ferrite-based magnetic fluids for hyperthermia applications. J. Biomed. Mater. Res. B Appl. Biomater. 2007; 81(1):12–22. [PubMed: 16924619]
3. Morana G, Salviato E, Guarise A. Contrast agents for hepatic MRI. Cancer Imaging. 2007 7 Spec No A:S24-7.
4. Gazuea F, Levy M, Wilhelm C. Optimizing magnetic nanoparticle design for nanothermotherapy. Nanomedicine. 2008; 3(6):831–844. [PubMed: 19025457]
5. Jordan A, Scholz R, Wust P, et al. Endocytosis of dextran and silan-coated magnetite nanoparticles and the effect of intracellular hyperthermia on human mammary carcinoma cells in vitro. J. Magn. Magn. Mater. 1999; 194:185–196.
6. Clifton KH, Drapers NR. Survival-curves of Solid Transplantable Tumour Cells Irradiated in Vivo: A Method of Determination and Statistical Evaluation; Comparison of Cell-survival and 32P-uptake into DNA. Int. J. Rad. Bio. 1963; 7(6):515–535.

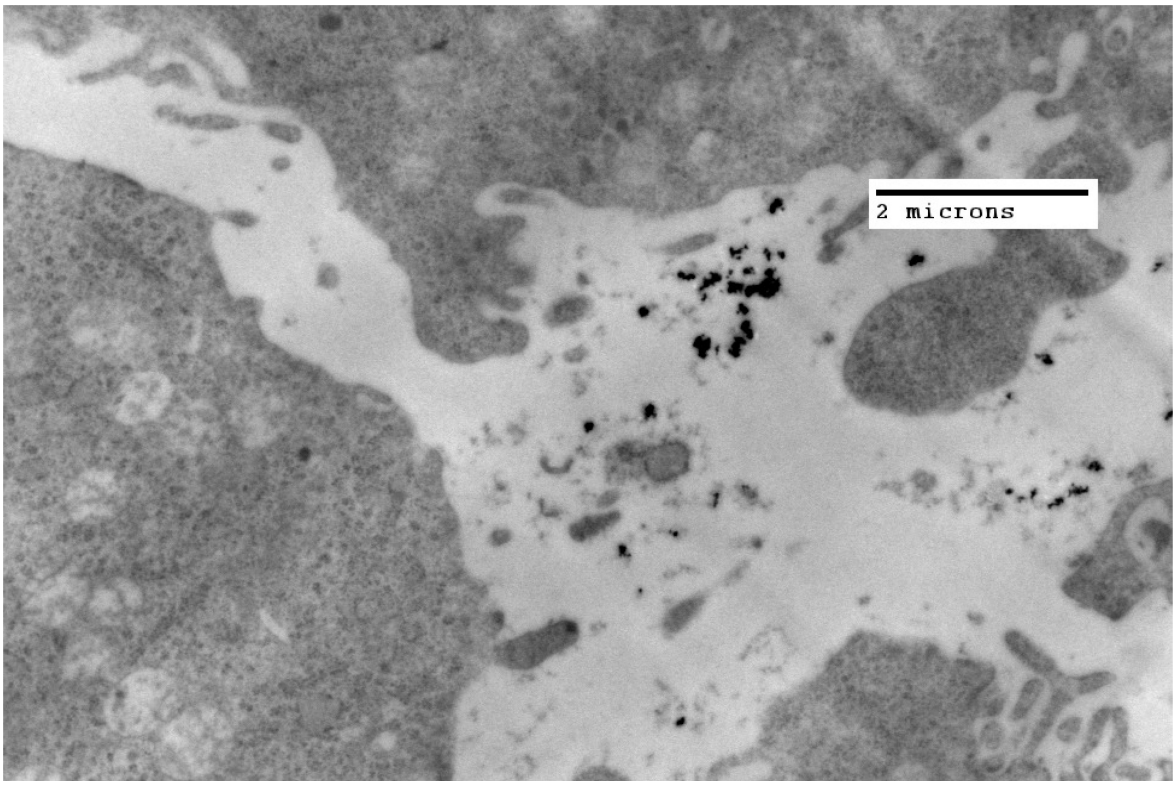


**Figure 1.**
TEM image of MTG-B tumor fixed in glutaraldehyde 1 hour post injection of 100 nm IONPs into a syngeneic tumor. All of the nanoparticles seen within this specimen are in the extracellular space.

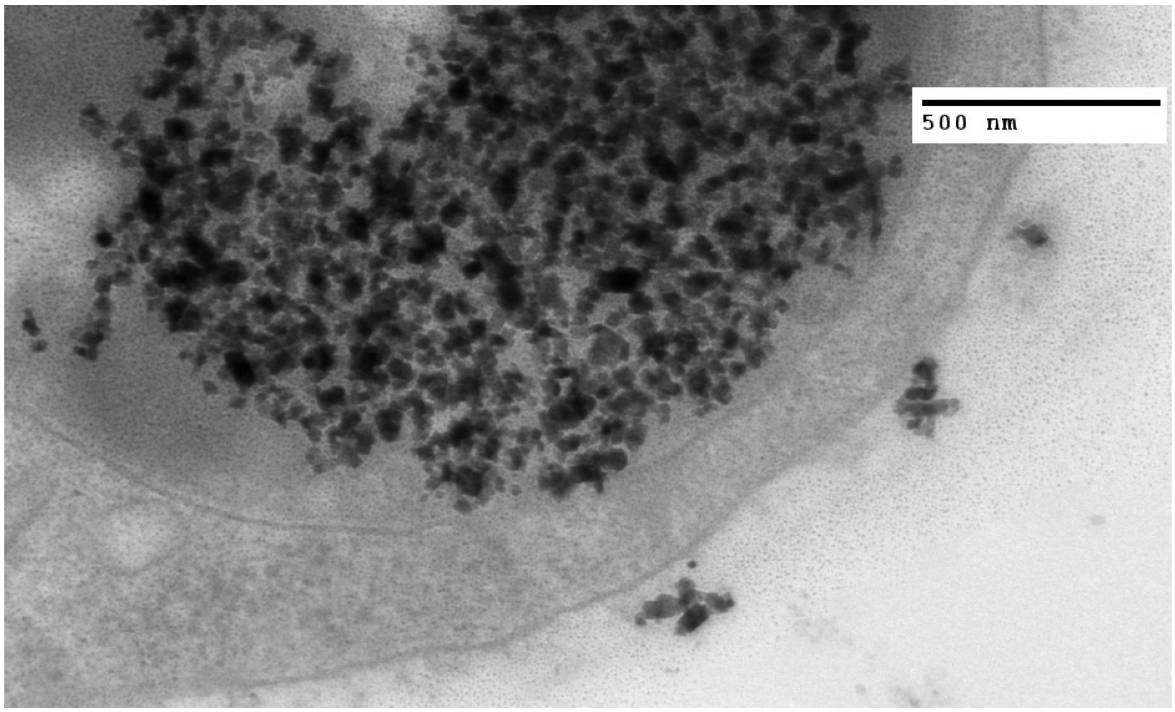


**Figure 2.**

TEM image of MTG-B tumor fixed in glutaraldehyde three hours post injection of 100 nm iron oxide nanoparticles into the tumor. Nanoparticles are seen both within and outside of the cell. Three hours appears approximately to be the time at which nanoparticles transition from being predominantly present outside of the cells to present within MTG-B cells.

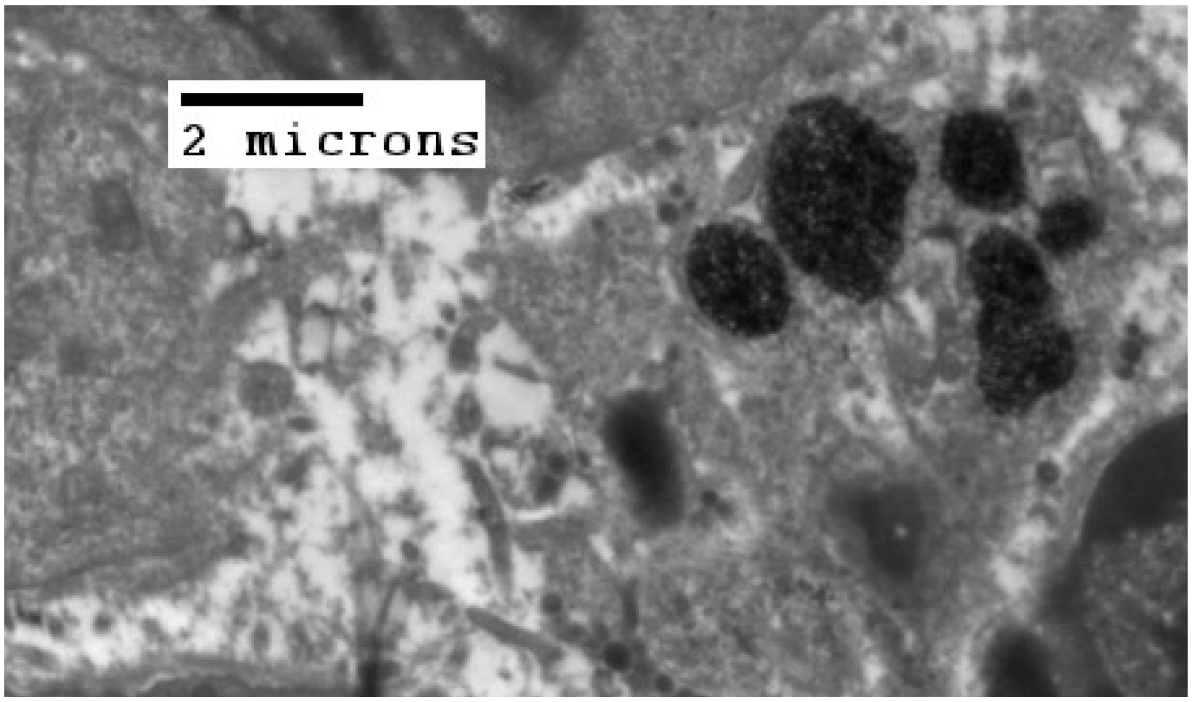


**Figure 3.**
TEM image of MTG-B tumor fixed in glutaraldehyde four hours after injection of nanoparticles into the tumor. At four hours post injection, few nanoparticles are seen outside of cells and numerous cytoplasmic vesicles containing many IONPs are seen within the cells.

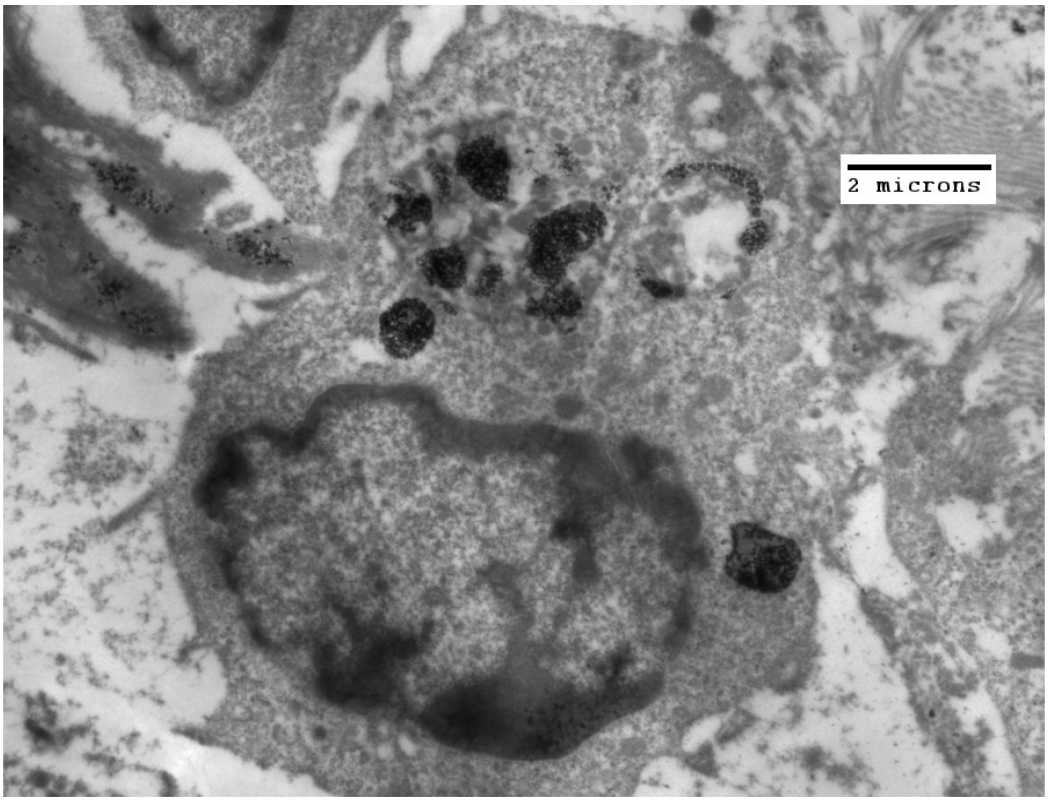


**Figure 4.**
TEM of MTG-B tumor fixed in glutaraldehyde 22.5 hours post injection of nanoparticles into the tumor. At incubation times greater than three hours in MTG-B tumors, few nanoparticles are seen outside of cells. There appears to be little difference in IONP particle position in MTG-B tumors with four or more hours of incubation post-injection.

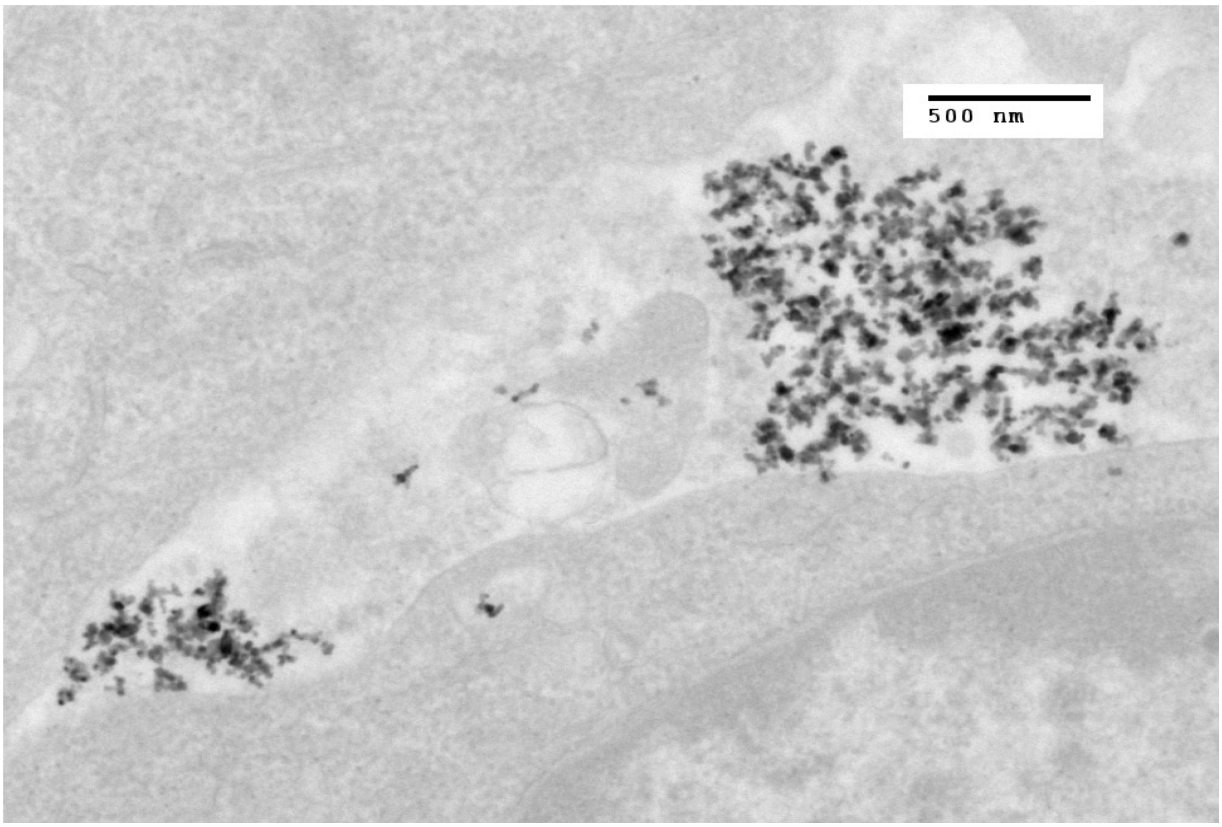


**Figure 5.**
TEM of HT-29 tumor fixed in glutaraldehyde four hours after injection of nanoparticles into the tumor. By four hours post injection, few nanoparticles are seen inside of cells. This information demonstrates the significant potential differences in IONP uptake for various tumor types.

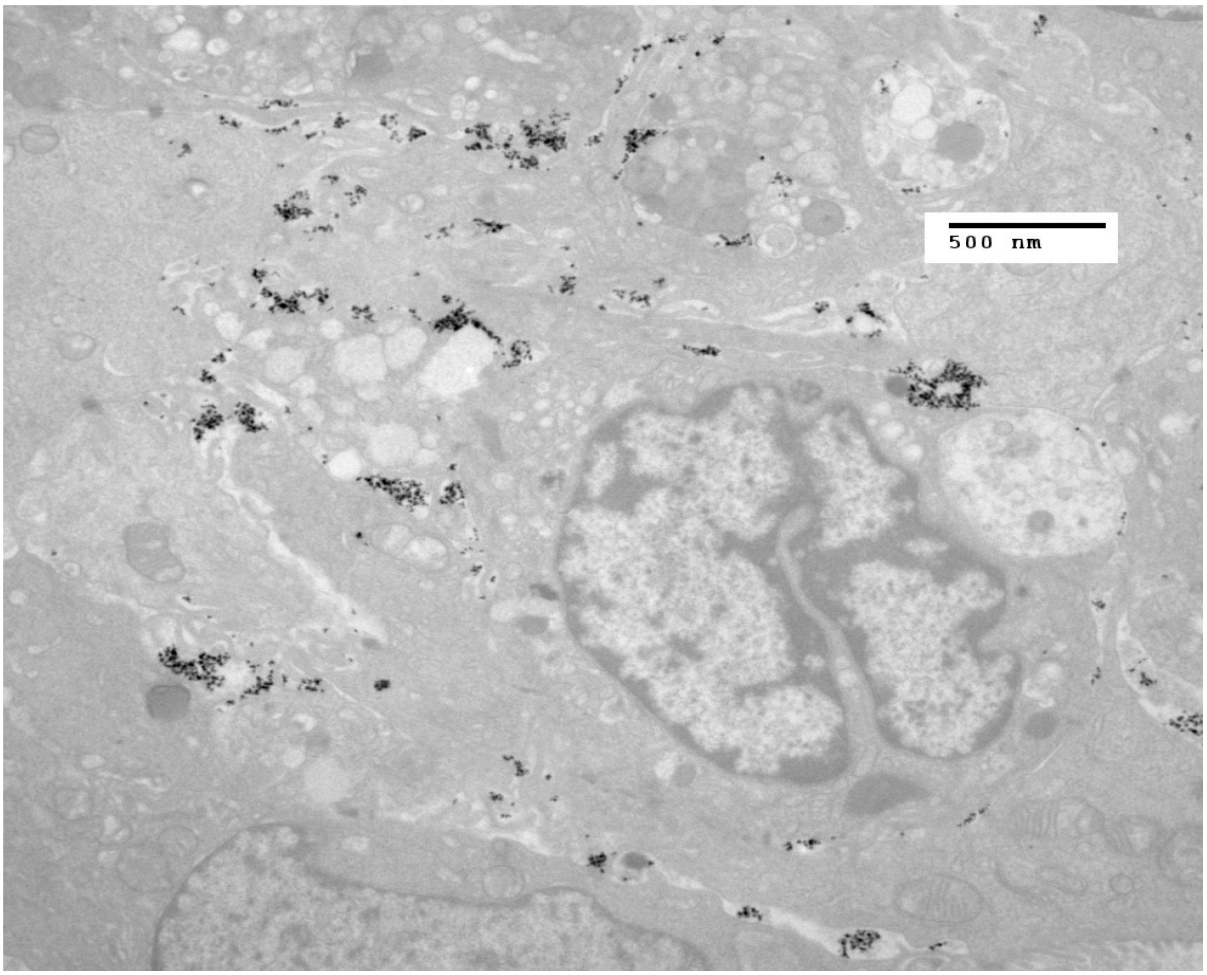


**Figure 6.**
Another TEM of HT-29 tumor fixed in glutaraldehyde four hours after injection of nanoparticles into the tumor. By four hours post injection, few nanoparticles are seen inside of cells.